Observation of the electron-hole liquid in $Si_{1-x}Ge_x/Si$ quantum wells by steady-state and time-resolved photoluminescence measurements

V. S. Bagaev,[1] V. S. Krivobok,[1,2,*] S. N. Nikolaev,[1,2] A. V. Novikov,[3] E. E. Onishchenko,[1] and M. L. Skorikov[1]
[1]*P.N. Lebedev Physical Institute, Russian Academy of Sciences, Moscow, Russia*
[2]*Moscow Institute of Physics and Technology (State University), Dolgoprudny, Moscow Region, Russia*
[3]*Institute for Physics of Microstructures, Russian Academy of Sciences, Nizhny Novgorod, Russia*
(Received 19 July 2010; published 20 September 2010)

The formation of quasi-two-dimensional electron-hole liquid in a $Si_{0.95}Ge_{0.05}/Si$ quantum-well structure was observed by steady-state and time-resolved photoluminescence measurements. In the temperature range 2–15 K, the main characteristics of the liquid phase (e.g., the equilibrium concentration of 1.0×10^{12} cm^{-2} and lifetime of 400 ns) remain unchanged. However the nature of the related excitonic gas-liquid transition depends on the temperature and the disorder in the system.

DOI: 10.1103/PhysRevB.82.115313 PACS number(s): 78.67.De, 71.10.Pm, 71.35.Ee, 73.21.Fg

I. INTRODUCTION

Since being predicted by Keldysh more than four decades ago, the phenomenon of exciton condensation into droplets of metallic electron-hole liquid (EHL) has been the subject of intense research efforts.[1] In contrast to ordinary electron-hole plasma (EHP) EHL has a fixed equilibrium density and a sharp border separating it from excitonic gas. Studies on the EHL in three-dimensional (3D) systems provided the basis that allows verification of many-body theories dealing with interacting Fermi particles.[2] With the appearance of two-dimensional (2D) semiconductor structures, it became important to investigate the possibility of exciton condensation, properties of the condensed phase, and the nature of the gas-liquid transition in 2D systems. Interest in these studies is related, in particular, to the basic difference between the screening-induced collapse of 2D and 3D excitonic states. It is well known that for the 2D case a bound state exists in an arbitrarily weak localizing potential; i.e., although screening of the Coulomb interaction reduces both the binding energy and oscillator strength of the exciton, it cannot destroy the excitonic state. Furthermore, the character of the screening itself as well as the filling factors of electron and hole states in a degenerate Fermi liquid are modified for low-dimensional systems.[3]

A question of major importance related to phase transitions in a system of excitons and free carriers concerns the deviation of this system from thermodynamic equilibrium and its effect on the character of the transition observed (see, e.g., Ref. 4). Indirect-gap semiconductor structures, where exciton lifetimes are long owing to the momentum selection rules, are promising in this context. Evidence for the existence of the EHL in indirect-gap semiconductor quantum wells (QWs) has been reported recently for Si/SiO_2 structures.[5] But the main results of these studies are related to phase transitions in a quasi-3D system of nonequilibrium electrons and holes with a rather weak spatial confinement. For structures with thinner wells, where quantum confinement occurs, the analysis of phase separation in the photoexcited electron-hole system seems to be very difficult since their photoluminescence (PL) spectra exhibit only a broad structureless band in the entire temperature range investigated. A promising kind of system for investigating phase transitions between the excitonic gas and the EHL and the excitonic gas and the EHP are $Si_{1-x}Ge_x/Si$ QWs with low germanium content ($x<0.1$).[6–8] In contrast to QWs based on direct-gap semiconductors, the lifetimes of excitons and free carriers in high-quality SiGe/Si structures fall into the submicrosecond range, which is long enough for efficient thermalization even at liquid-helium temperatures. At the same time, for low x the conduction-band offset is sufficiently small as compared to the Coulomb attraction of electrons and holes in the SiGe layer, and one expects that confined excitons attain spatially direct character (in contrast to structures with higher germanium content[9]). The goal of this paper is to demonstrate the possibility of the EHL formation and to study the main features of quasi-2D exciton condensation in thin $Si_{1-x}Ge_x/Si$ QWs with $x\simeq0.05$.

II. EXPERIMENT

The samples under study were grown by molecular-beam epitaxy on boron-doped Si(100) substrates and consisted of a 100-nm-thick Si buffer layer, a SiGe layer and a 100-nm-thick Si cap layer. Schematic overview of the band alignment in such structures is presented in the inset of Fig. 1. High-resolution x-ray analysis and preliminary low-temperature photoluminescence measurements allowed us to estimate the Ge content in SiGe layers and to characterize the structural quality of the samples.[10] For the present study we selected one of the highest-quality samples, comprising a 5-nm-thick $Si_{0.95}Ge_{0.05}$ layer; its homogeneity is attested to by the very small width (below 1 meV) of the QW exciton PL line observed at the lowest excitation levels. In such a structure, there exists an approximately 40-meV-deep potential well for holes in the SiGe layer with the heavy-hole subband being the ground one,[10] and confinement of electrons occurs mainly because of their Coulomb attraction to holes. For the PL measurements, the samples were mounted in a cryostat and were either immersed in superfluid helium or blown by helium vapors. Different cw and pulsed lasers were used for the PL excitation. Depending on specific experiments, cw laser radiation was focused to a spot 0.2–5.0 mm in diameter. In order to eliminate the effect of the exciton diffusion on the

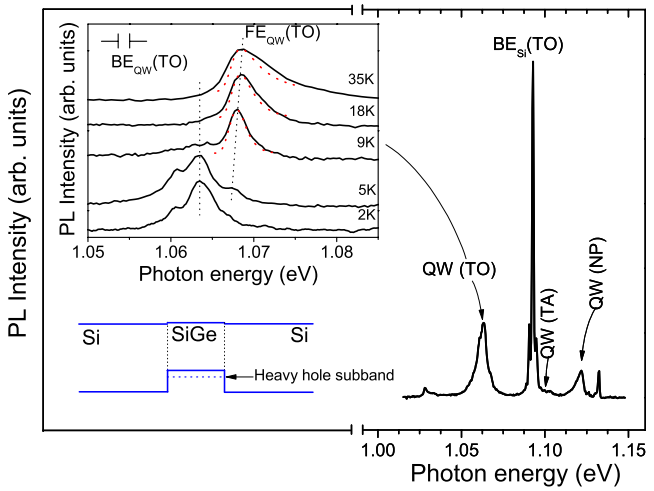

FIG. 1. (Color online) A survey PL spectrum of the $Si_{0.95}Ge_{0.05}$ structure under study at a moderate level of the Ar^+-laser excitation (0.1 W/cm^2) and $T=5$ K. The upper inset shows a changeover from the bound exciton (BE_{QW}) to the free exciton (FE_{QW}) line in the PL spectra of the QW as the temperature increases (excitation density 0.01 W/cm^2); dashed lines show fits of the FE_{QW} PL line according to Eq. (1). Inset in the bottom reproduces schematic overview of band alignment in a $Si_{1-x}Ge_x$ QW (Ref. 9).

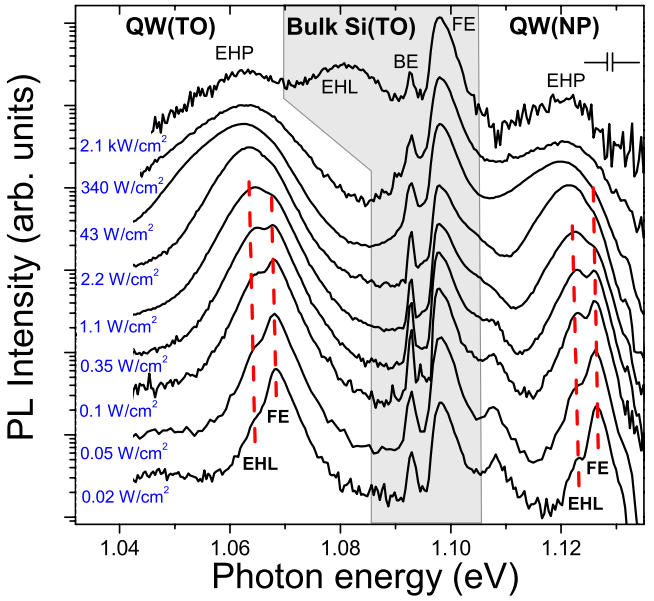

FIG. 2. (Color online) Formation of the EHL in the QW and then in bulk silicon with increasing level of the Ar^+-laser excitation at $T=15$ K.

recorded PL kinetics, the excitation spot of pulsed laser was kept sufficiently large (~5 mm). PL spectra were recorded by a grating spectrometer equipped with a cooled Ge detector (Edinburg instruments L990602); a photomultiplier which enabled about 15 ns time resolution was used for kinetic measurements (see Ref. 11 for details). Weak emission in the visible range was recorded by a cooled charge coupled device matrix detector.

III. RESULTS AND DISCUSSION

The PL spectrum of the structure under study recorded at a temperature $T=5$ K is presented in Fig. 1. The QW spectrum consists of no-phonon (NP) transitions in the region 1.110–1.125 eV and transitions accompanied by the emission of transverse-optical (TO), longitudinal-optical (LO), and transverse-acoustic (TA) phonons corresponding to the X point in the Brillouin zone of silicon.[12] It should be noted that strong quenching of the overall emission from the QW was observed at $T>35$ K. In addition to the QW lines, the PL spectrum in Fig. 1 reveals the emission of bulk Si (substrate as well as buffer and cap layers) related to impurity bound excitons (BE_{Si}), which transforms into the emission of free excitons (FE_{Si}) at higher temperatures. The latter are characterized by relatively long lifetimes τ and diffusion lengths L_d (at 15 K $\tau=950$ ns and $L_d \sim 0.5$ mm, which is comparable to the sample thickness of 450 μm).

The inset in Fig. 1 shows the fine structure of the QW emission in the region of LO/TO phonon replicas (hereafter marked TO for brevity) recorded at low excitation density and different temperatures. This fine structure demonstrates a changeover from bound excitons (BE_{QW}) to free excitons (FE_{QW}) in the QW as the temperature increases. Quenching of the BE_{QW} emission occurs already at ~10 K. Furthermore, as the temperature increases the FE_{QW} line exhibits a blueshift of approximately 0.06 meV/K, which is induced by the fluctuations in the confinement potential of the QW. Under the assumption of full exciton thermalization in the QW, the FE_{QW} line shape can be approximated by the following expression:[13]

$$I(\hbar\omega) \sim \left[1 - \mathrm{erf}\left(\frac{E_0 - \hbar\omega}{\sqrt{2}\sigma}\right)\right] \cdot \exp\left(-\frac{E_0 - \hbar\omega}{kT}\right). \quad (1)$$

Here, σ stands for the dispersion in the energy of the QW excitonic band bottom with respect to its average value E_0, T is the effective temperature of excitons, and erf(x) denotes the error function. Fitting the recorded spectra according to Eq. (1), we obtain an estimate on the magnitude of the potential fluctuations in the QW $\sigma \sim 0.3$–0.4 meV, which is comparable to the thermal energy at 5 K. This implies that, at $T \sim 5$ K and below, the fluctuations of the excitonic band bottom have a noticeable effect on the behavior of excitons in the QW and the related PL spectra, while at temperatures significantly higher than 5 K these fluctuations can be treated as a perturbation. Thus, it follows from the foregoing discussion that the temperature range 10–35 K is the best suited for the observation of phase transitions occurring in the QW.

Figure 2 shows the evolution of the PL spectra at 15 K with increasing excitation density. The bulk Si emission demonstrates a classical excitonic gas-liquid transition accompanied by the formation of the EHL, typical of unstrained Si. The main effect of the excitation power increase on the QW emission is the appearance of new satellites on the low-energy side of the FE_{QW}(NP) and FE_{QW}(TO) lines, which can be seen at excitation densities as low as ~0.05 W/cm^2. These satellites dominate the PL spectra of the QW at excitation densities of 0.5 W/cm^2 and higher.

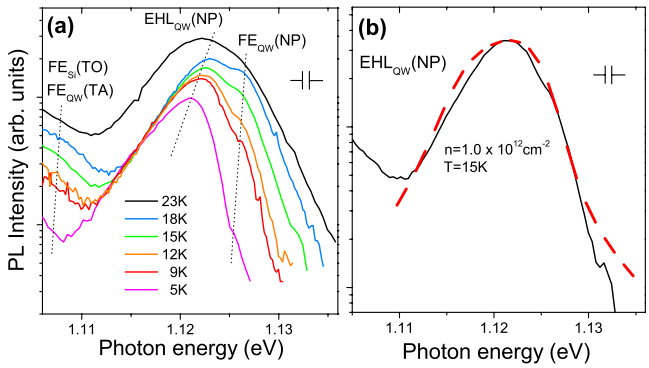

FIG. 3. (Color online) (a) The PL spectra in the region of the no-phonon QW emission band at an excitation density of ~1 W/cm^2 and different temperatures, indicated in the figure. The low-energy tail of the EHL$_{QW}$(NP) component is invariant in the temperature range 5–18 K. (b) A fit (dashed line) of the EHL$_{QW}$(NP) emission band at 15 K described in the text.

The corresponding doublet structure observed in the excitation range 0.05–2 W/cm^2 is an evidence of two separate mechanisms of radiative recombination in the QW. As the excitation density is raised still higher, the FE$_{QW}$(NP) and FE$_{QW}$(TO) lines disappear from the spectrum and the width of the QW emission band increases steadily.

The radiative recombination governed by collective effects for the system of free particles in semiconductor structures is commonly attributed to the following processes: (1) recombination of free-multiexciton complexes (MECs) and trions;[2,14,15] (2) inelastic exciton-electron, exciton-hole, and exciton-exciton scattering;[14,16] (3) recombination in EHP;[2,14,16] and (4) recombination in EHL.[2,5,7]

The shape of the low-energy tail of an emission band originating from processes (1) and (2) is typically determined by the energy and momentum conservation requirements and depends strongly on the temperature of the system.[14–17] Meanwhile, according to Fig. 3(a), the low-energy tail of the QW emission band at an excitation density 1 W/cm^2 remains approximately the same in a wide temperature range. Moreover, processes (1) and (2) usually exhibit superlinear behavior with the excitation density, which we failed to observe in our experiments. For the EHP recombination [process (3)], both the shape and position of the emission band depend substantially on the excitation density owing to the variation in the electron (μ_e) and hole (μ_h) quasi-Fermi levels and the band-gap renormalization.[2,14] In the case of the EHL, an increase in the excitation density does not result in the variation in μ_e and μ_h, leading instead to an increase in the volume of the condensed phase. As a consequence, the shape and position of the emission band are stabilized while the related PL intensity grows approximately linear with the excitation intensity. It is just this behavior that we observe in the QW spectra shown in Fig. 2 for the excitation range 0.1–2 W/cm^2 [nevertheless it should be noted that the QW emission at excitation densities of ~0.1 W/cm^2 and lower can be contributed by both EHL and free MEC (Ref. 8)]. Furthermore, in the case of the EHL, the low-energy tail of the emission band is characterized by weak temperature dependence for $kT \ll \mu_e + \mu_h$, which is in perfect agreement with the data in Fig. 3(a).

Quantitative information concerning the main characteristics of the confined EHL can be deduced from the line-shape analysis. In general, this analysis should take into account inhomogeneities of the structure as well as homogeneous broadening caused by the fact that, upon recombination of an electron with a hole, the EHL finds itself in an excited state with a short lifetime.[13] However, to a first approximation, the effect of inhomogeneities can be neglected, insofar as the half width of the EHL emission band (which is determined by the sum of the quasi-Fermi levels $\mu_e + \mu_h$) is much larger than the magnitude of inhomogeneous broadening σ. In the framework of this approximation, the shape of the EHL$_{QW}$ emission band can be successfully fitted if one takes into account the finite width of the EHL excited states, which governs the low-energy tails in the PL spectra.[6,13] In this case the line shape of EHL emission band can be described by the following formulas:[18]

$$I(\hbar\omega) = I_0 \int_0^\infty \int_0^\infty \rho_C(E_C)\rho_V(E_V) f_C(E_C) f_V(E_V) \times \frac{1}{2\pi} \frac{\Gamma(E_C,E_V) dE_C dE_V}{(\hbar\omega - E_V - E_C - \Delta)^2 + \Gamma^2(E_C,E_V)/4}. \quad (2)$$

Here, $\Gamma(E_C,E_V)$ is the half width of the excited states formed in the electron-hole plasma after the recombination of an electron and a hole with the energies E_C and E_V, respectively (the energy is reckoned from the edges of the corresponding bands of the quantum well), and Δ is the renormalized band gap. The experimental data were approximated using Eq. (2) within the model of a two-dimensional electron-hole plasma with the effective (lateral) masses of the density of electron states $m_e = 4(m_\parallel m_\perp)^{1/2} = 1.68 m_0$ and holes states $m_h = 0.21 m_0$,[19] which determine the two-dimensional (independent of the energy) density of states $\rho_C(E_C)$ and $\rho_V(E_V)$. Here, $f_C(E_C)$ and $f_V(E_V)$ are the Fermi distribution functions with the quasi-Fermi levels of electrons and holes μ_e and μ_h dependent on the plasma density $n_e = n_h \equiv n$ and the temperature T;[20] that is,

$$\mu_{e,h} = kT \ln\left(\exp\frac{\pi\hbar^2 n}{m_{e,h} kT} - 1\right). \quad (3)$$

The dashed line in Fig. 3(b) represents the result of such a fit carried out as described in Ref. 6. In this fit, the temperature of electrons and holes in the EHL was not varied and assumed to be equal to the temperature of free excitons in bulk Si. The resulting electron-hole pair density in the EHL was estimated to be $n \simeq 1.0 \times 10^{12}$ cm^{-2} with an error of approximately 10%. This error is the result of ignoring the inhomogeneous broadening and weak indeterminable contribution of the FE$_{QW}$ line.

Additional evidence of the EHL formation can be deduced from the analysis of the QW PL decay kinetics. Figure 4 illustrates PL decays corresponding to different spectral positions within the no-phonon QW emission band at 15 K. These positions are marked in the inset of Fig. 4 where stationary PL spectra recorded at the excitation densities 0.02, 1.1, and 340 W/cm^2 (from bottom to top) are shown. Note a qualitative difference in the kinetics of the PL related to free

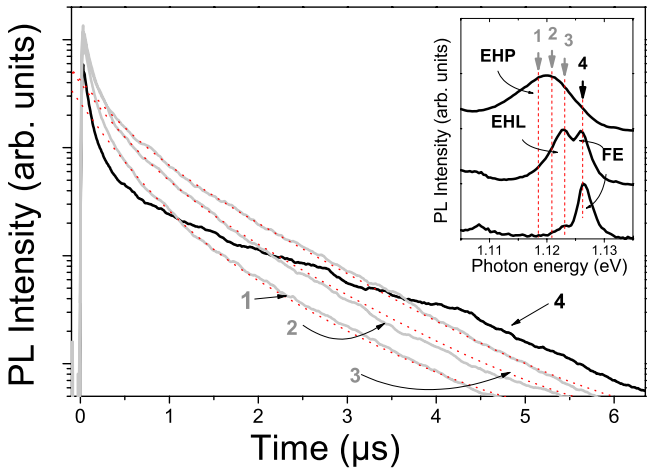

FIG. 4. (Color online) PL kinetics recorded at 15 K at several spectral points (indicated in the inset) corresponding to FE_{QW}(NP) (curve 4) and EHL_{QW}(NP) (curves 1–3) emission. Dotted lines are two-exponential fits described in the text.

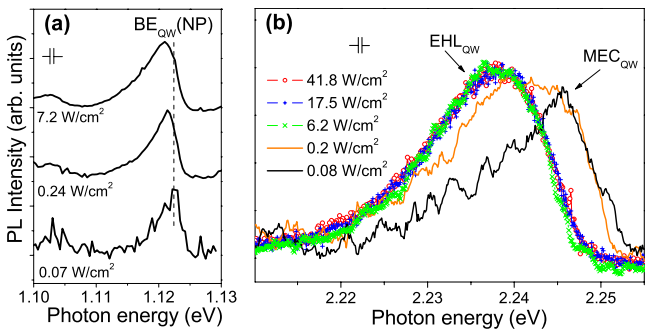

FIG. 5. (Color online) PL spectra of the QW at 2 K in the visible and infrared regions. (a) QW (NP) emission band recorded at different levels (0.07–7 W/cm^2) of the excitation by an Ne^+ laser (λ=0.35 μm). Ultraviolet excitation with low penetration depth was used to suppress formation of the EHL in bulk Si and reduce the contribution from EHL_{Si}(TA) replica, which appears close to the QW_{SiGe}(NP). (b) $2E_g$ PL spectra recorded at different levels of the excitation by a Ti-sapphire laser (λ=0.78 μm), revealing different many-particle states in the QW.

excitons (curve 4) and different regions of the band caused by many-particle interaction (curves 1–3). The fact that curves 1–3 run parallel to each other in the range of times ~950 ns after the excitation pulse and longer confirms the conservation of the PL band shape. For a detailed analysis of the PL kinetics it is important to take into consideration efficient injection of excitons into the QW due to their capture from the barriers. As the diffusion length of "bulk" excitons at 15 K is long enough, the rate of the exciton injection into the QW should be approximately proportional to the concentration of free excitons in bulk Si. Now, if several independent channels of recombination in the QW are characterized by time constants t_i and the injection rate decays exponentially with a time constant t_0, the resulting kinetics of the QW PL should represent a sum of exponential decays with time constants t_i and t_0. The evolution of curves 1–3 in Fig. 4 at times longer than ~500 ns after the excitation pulse is described by just two exponential components with time constants t_0=950 ns and t_1=400 ns. The time constant t_0 agrees well with the lifetime of free excitons in bulk Si at 15 K, which confirms the interconnection of the PL kinetics related to the bulk and the QW. The other time constant t_1 =400 ns characterizes processes taking place in the QW only. The corresponding exponential decay can be more clearly observed in the time range 0.5–5.5 μs after the excitation pulse when the component describing the FE_{Si} decay is subtracted from curves 1–3 in Fig. 4. Fast nonexponential decays observed in Fig. 4 just after an excitation pulse seems to be related with a dense EHP in the QW. But the indeterminable injection rate of excitons complicates a sophisticated study of PL kinetic in the time range of 0–500 ns.

For indirect semiconductors, the lifetime of charge carriers is usually determined by Auger-type recombinations and depends substantially on the carrier concentration.[2] Exciton recombination accompanied by inelastic scattering also becomes less important as the concentration decreases. Thus, the carrier lifetime in the QW should increase steadily after the excitation pulse if recombination occurs in the EHP or the excitonic gas. In the case of the EHL, fixed concentration of carriers ensures stabilization of the PL decay time, and this behavior is observed in the recorded kinetic curves in the range of times longer than ~500 ns after the excitation pulse. Finally, a kink observed in the FE_{QW}(NP) PL decay (curve 4) cannot be explained in the context of purely exciton or MEC recombination but finds natural explanation in the picture of coexisting excitons and EHL: it is a consequence of the EHL evaporation, well known for bulk semiconductors.[2]

As the temperature decreases, stability of a degenerate EHL with respect to the excitonic gas is enhanced owing to the much less pronounced temperature dependence of the chemical potential in the liquid phase. However, interpretation of the PL spectra recorded at low temperatures is complicated by the presence of an intense BE line and, at higher excitation levels, lines of localized MEC in the QW. One can see from Fig. 5(a), that, at any excitation used, the QW emission at 2 K is represented by a structureless band and the most noticeable transformation of the spectrum occurs at the low-energy tail of this band.

A direct experiment clarifying the existence of the EHL emission lines at low temperatures can be based on the excitation-power dependence of the PL spectra in the range 2.1–2.3 eV (so-called $2E_g$ luminescence[21]). The PL in this spectral region does not include the emission originating from free and bound excitons, as the $2E_g$ luminescence is governed by simultaneous recombination of two electrons from opposite valleys and two holes resulting in the emission of a single photon. The excitation-power dependence of the $2E_g$ PL spectra of the QW under study at 2 K is presented in Fig. 5(b). In contrast to the IR spectra [Fig. 5(a)], the $2E_g$ luminescence exhibits a structure demonstrating the existence of different many-particle states in the QW. At a relatively low excitation density ($W \sim 0.08$ W/cm^2), there is an asymmetric line at 2.246 eV. The shape and position of this line, close to the doubled energy of the excitonic band bottom (2.249 eV), suggest that it is related to MEC. An increase in the excitation-power density to several watts per

square centimeter results in the appearance of a new broad band at 2.238 eV. As the power is still raised further, the high-energy component disappears while the shape and position of the low-energy band remains unchanged with increasing excitation level. The PL kinetics recorded for the corresponding spectral position in the IR region reveals a decay time of ~400 ns, which agrees well with the lifetime of e-h pairs in the EHL measured at 15 K.

Thus, the experimental data obtained confirm the existence of the EHL in the QW at $T=2$ K. But the pattern of the EHL formation seems to be different from that observed at higher temperatures. According to Fig. 5, an increase in the excitation level leads to gradual changes governed mainly by the growth of MEC. Behavior typical of the EHL (i.e., fixed e-h density and binding energy) sets in only at relatively high excitation densities when the contribution from MEC is negligible. It may be possible that, in this case, thresholdless condensation of carriers loses the characteristic features of a first-order phase transition.

IV. CONCLUSION

In conclusion, the formation of EHL with the concentration of electron-hole pairs $\sim 1.0\times 10^{12}$ cm^{-2} and the carrier lifetime ~400 ns in a thin (5 nm) $Si_{0.95}Ge_{0.05}/Si$ QW at liquid-helium temperatures is demonstrated. The character of the corresponding gas-liquid phase transition depends substantially on the ratio σ/kT, where σ is the disorder-induced broadening of excitonic states and kT is the thermal energy. At temperatures satisfying the condition $\sigma \ll kT$ but sufficiently low to make possible the EHL formation, the system exhibits coexistence of excitons and EHL, which is a signature of a first-order phase transition. In this case, evaporation of excitons from the EHL to the gas phase shows up in the kinetics of the QW emission. At lower temperatures, when $kT \lesssim \sigma$, the system does not exhibit a well-defined coexistence of distinct phases typical of first-order phase transitions at any excitation density used. In this case the EHL formation is governed by a gradual transformation from bound excitons to bound MEC and then to the EHL.

ACKNOWLEDGMENTS

We are grateful to T. M. Burbaev and N. N. Sibeldin for useful discussions of the issues involved. This study is supported by the RFBR (Project No. 09-02-01233).

*krivobok@lebedev.ru

[1] N. N. Sibeldin, *Quantum Coherence Phenomena in Electron-Hole and Coupled Matter-Light Systems*, Problems of Condensed Matter Physics Vol. 139 (Oxford University Press, New York, 2008), pp. 227–257.
[2] *Electron-Hole Droplets in Semiconductors, Modern Problems in Condensed Matter Sciences*, edited by C. D. Jeffries and L. V. Keldysh (North-Holland, Amsterdam, 1983).
[3] H. Reinholz, Solid State Commun. **123**, 489 (2002).
[4] L. Kappei, J. Szczytko, F. Morier-Genoud, and B. Deveaud, Phys. Rev. Lett. **94**, 147403 (2005).
[5] N. Pauc, V. Calvo, J. Eymery, F. Fournel, and N. Magnea, Phys. Rev. B **72**, 205324 (2005).
[6] V. S. Bagaev, V. V. Zaitsev, V. S. Krivobok, D. N. Lobanov, S. N. Nikolaev, A. V. Novikov, and E. E. Onishchenko, JETP **107**, 846 (2008).
[7] T. M. Burbaev, V. A. Kurbatov, M. M. Rzaev, N. N. Sibel'din, V. A. Tsvetkov, and F. Schäffler, JETP Lett. **85**, 331 (2007).
[8] T. M. Burbaev, M. N. Gordeev, D. N. Lobanov, A. V. Novikov, M. M. Rzaev, N. N. Sibeldin, M. L. Skorikov, V. A. Tsvetkov, and D. V. Shepel', Pis'ma Zh. Eksp. Teor. Fiz. **92**, 341 (2010).
[9] T. Baier, U. Mantz, K. Thonke, R. Sauer, F. Schäffler, and H.-J. Herzog, Phys. Rev. B **50**, 15191 (1994).
[10] V. S. Bagaev, V. S. Krivobok, V. P. Martovitsky, and A. V. Novikov, JETP **109**, 997 (2009).
[11] S. N. Nikolaev, V. S. Krivobok, A. Y. Klokov, and V. S. Bagaev, Instrum. Exp. Tech. **52**, 110 (2009).
[12] P. J. Dean, J. R. Haynes, and W. F. Flood, Phys. Rev. **161**, 711 (1967).
[13] J. Christen and D. Bimberg, Phys. Rev. B **42**, 7213 (1990).
[14] R. Cingolani and K. Ploog, Adv. Phys. **40**, 535 (1991).
[15] A. Esser, E. Runge, R. Zimmermann, and W. Langbein, Phys. Rev. B **62**, 8232 (2000).
[16] L. V. Kulik, A. I. Tartakovskii, A. V. Larionov, E. S. Borovitskaya, and V. D. Kulakovskii, JETP **85**, 195 (1997).
[17] K. Cho, Opt. Commun. **8**, 412 (1973).
[18] T. Stoica and L. Vescan, J. Appl. Phys. **94**, 4400 (2003).
[19] C. Penn, F. Schäffler, G. Bauer, and S. Glutsch, Phys. Rev. B **59**, 13314 (1999).
[20] S. Ben-Tabou de-Leon and B. Laikhtman, Phys. Rev. B **67**, 235315 (2003).
[21] T. Steiner, L. Lenchyshyn, M. Thewalt, J.-P. Noël, N. Rowell, and D. Houghton, Solid State Commun. **89**, 429 (1994).